Supplementary information

Developmental decrease of entorhinal gate disrupts prefrontal-hippocampal communication in immune-challenged DISC1 knockdown mice

Xu et.al

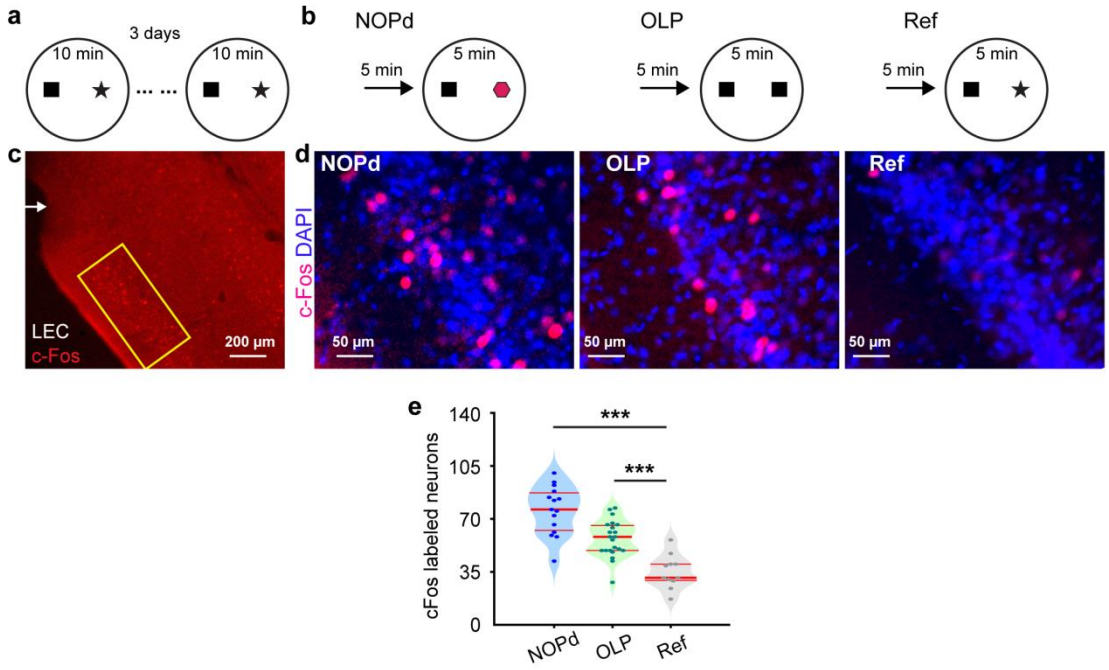

Supplementary fig.1 cFos immunoreactivity in LEC of mice tested in associative recognition tasks. (a) Schematic of the protocol for the familiarization trials (3 days, 2 trials per day). **(b)** Schematics of the protocol for NOPd test trial, OLP test trial, and reference trials (Ref). **(c)** Photomicrographs depicting cFos-expressing neurons (red) in the superficial layer of LEC from a P20 mouse, 90 mins after the test trial. **(d)** Photograph displaying the cFos-expressing cells (red dots) in LEC when stained for DAPI (blue) 90 mins after the NOPd test trial (left), OLP test trial (middle) and Ref trial (right). **(e)** Violin plots displaying the total number of cFos-positive neurons in the LEC of CON and GE mice (3~4 slices from 3 CON mice doing NOPd task, 3 CON mice doing OLP task, 2 CON mice doing Ref task). Single data points (i.e. the number of labeled neurons in LEC / slice) are shown as dots and the red horizontal bars in violin plots correspond to the median and the 25th and 75th percentiles. ***p<0.001.

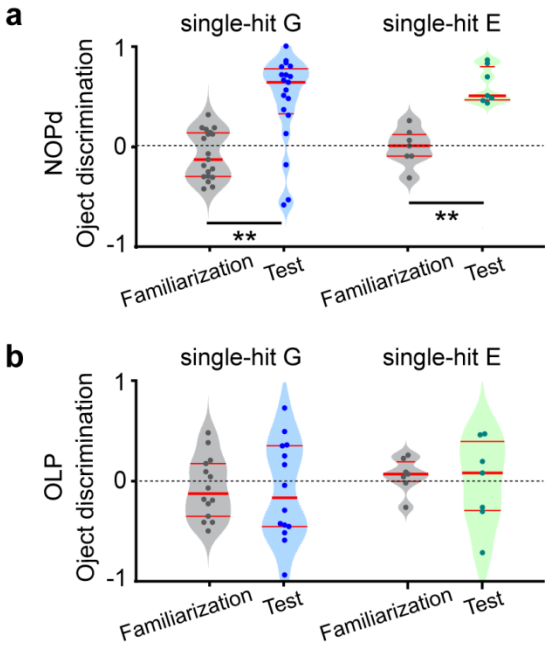

Supplementary fig.2 The performance of pre-juvenile single-hit G and E mice in associative recognition memory tasks. (a) Violin plots displaying the discrimination ratio in familiarization and test trials when averaged for single-hit G (DISC1 mice) and E (polyI:C-treated dams to induce MIA) mice. The black dotted line indicates chance level. **(b)** Violin plots displaying the discrimination ratio in familiarization and test trials when averaged for single-hit G and E mice. The black dotted line indicates chance level. Single data points are shown as dots and the red horizontal lines in violin plots correspond to the median and the 25th and 75th percentiles. **p<0.01.

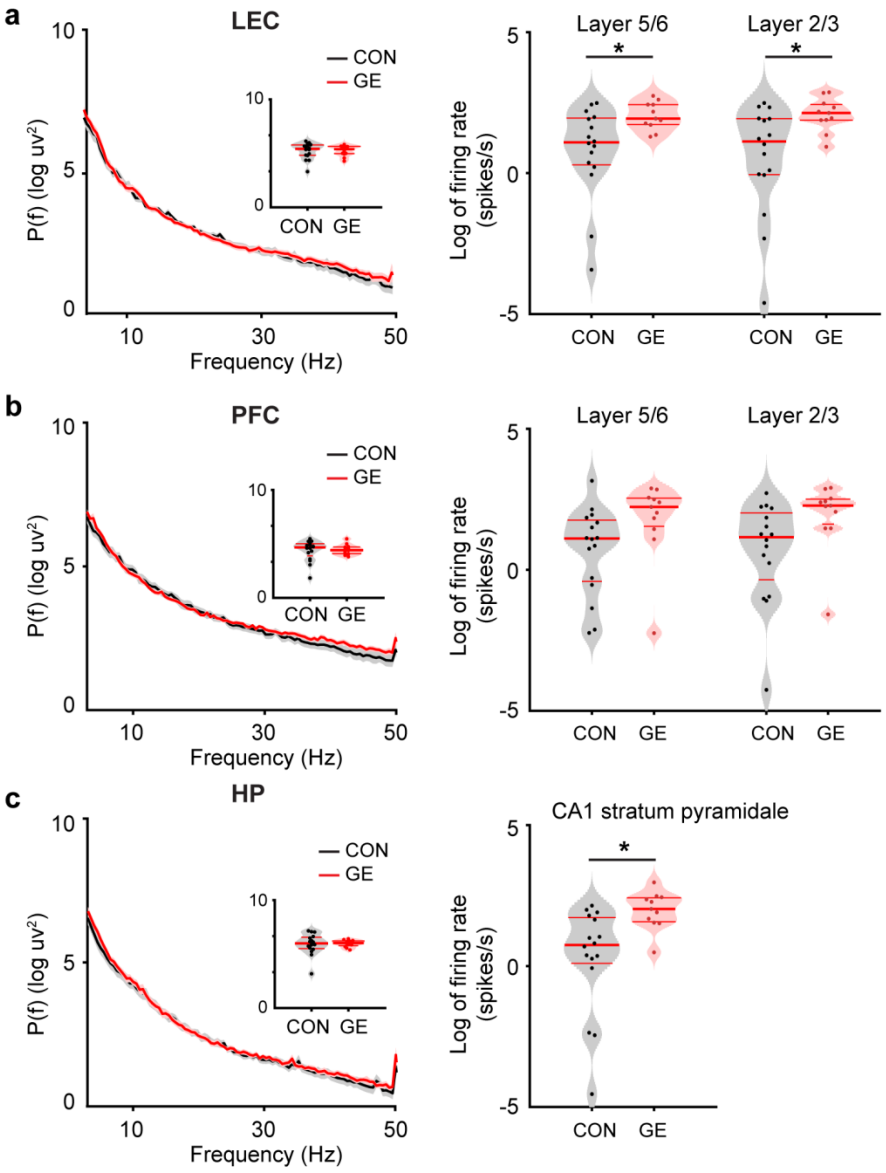

Supplementary fig.3 Patterns of network activity and neuronal firing in LEC, HP, and PFC from pre-juvenile CON and GE mice. (a) Averaged power spectra P(f) of oscillatory activity in CON and GE mice. Inset, violin plots displaying the average power spectra from 1-50 Hz in CON and GE mice. Right, violin plots displaying the firing activity of LEC neurons in CON and GE mice. **(b)** Same as **a** for PFC. **(c)** Same as **a** for HP. Single data points are shown as dots and the red horizontal bars in violin plots correspond to the median and the 25th and 75th percentiles. *p<0.05.

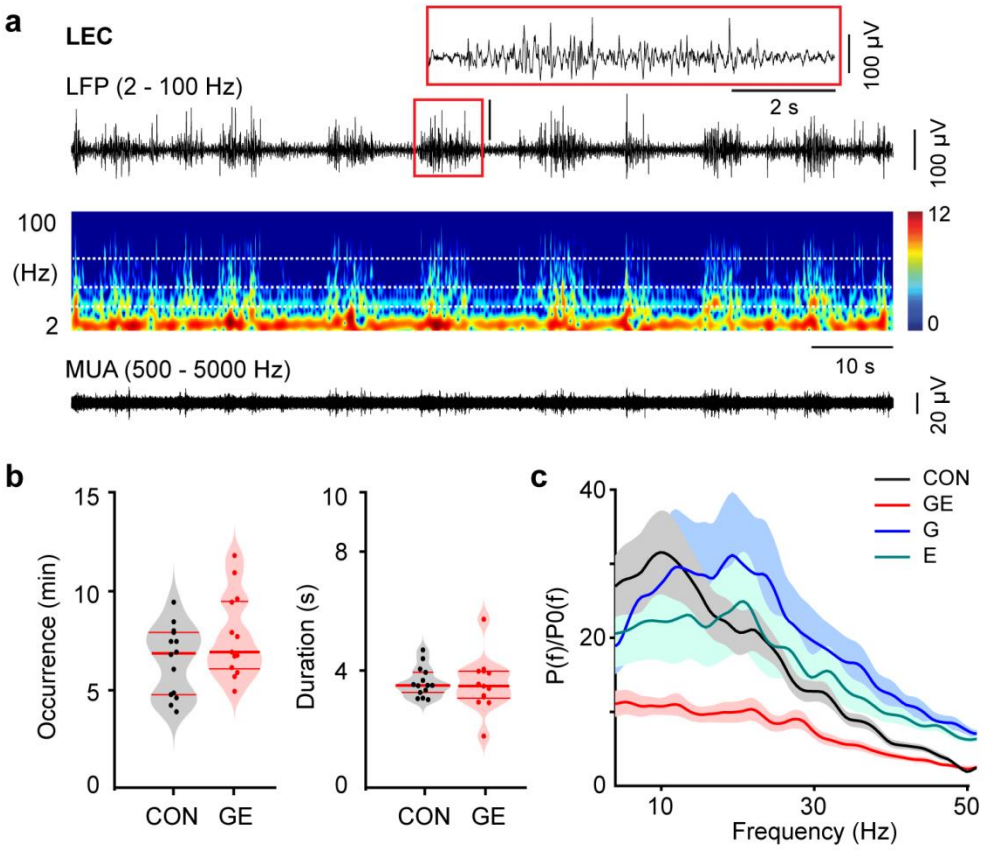

Supplementary fig.4 Patterns of network activity in the LEC of neonatal CON, GE, G, and E mice. (a) Extracellular LFP recordings of discontinuous oscillatory activity in the LEC from a P9 CON mice displayed after bandpass (2-100 Hz) filtering (top) together with the corresponding MUA after bandpass (500-5000 Hz) filtering (bottom). Traces are accompanied by the color-coded wavelet spectra of the LFP at identical time scale. **(b)** Violin plots displaying the occurrence and the duration of oscillatory activity in LEC recorded in CON and GE mice. **(c)** Averaged power spectra P(f) of discontinuous oscillatory activity normalized to the baseline power P0(f) of time windows lacking oscillatory activity in CON, double-hit GE, single-hit G and single-hit E mice. Single data points are shown as dots and the red horizontal bars in violin plots correspond to the median and the 25th and 75th percentiles.

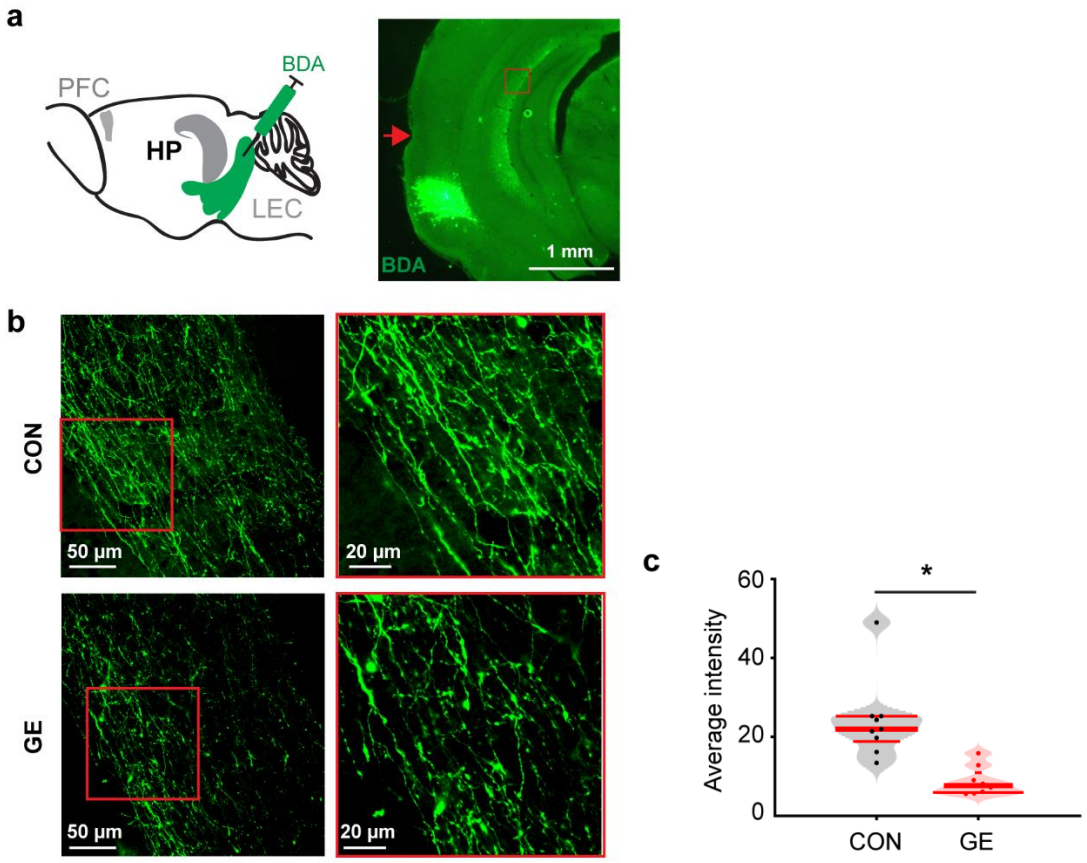

Supplementary fig.5 LEC axonal terminals in HP. (a) Schematic of the anterograde BDA injection in LEC. Right, photograph depicting the injection position in the LEC of a P10 CON mouse. The red arrow indicated rhinal fissure. The red square corresponds to the region used for the quantification of entorhinal terminals in HP. The red arrow corresponds to the rhinal fissure. **(b)** Left, photographs exemplarily illustrating entorhinal terminals in the HP of a P10 CON (top) and GE mice (bottom). Right, axonal terminals from the area marked by a red box shown at higher-magnification. **(c)** Violin plot displaying the averaged intensity of BDA in CON and GE mice. Single data points (i.e. the averaged intensity of BDA in HP per slice) are shown as dots and the red horizontal bars in violin plots correspond to the median and the 25th and 75th percentiles. *p<0.05.

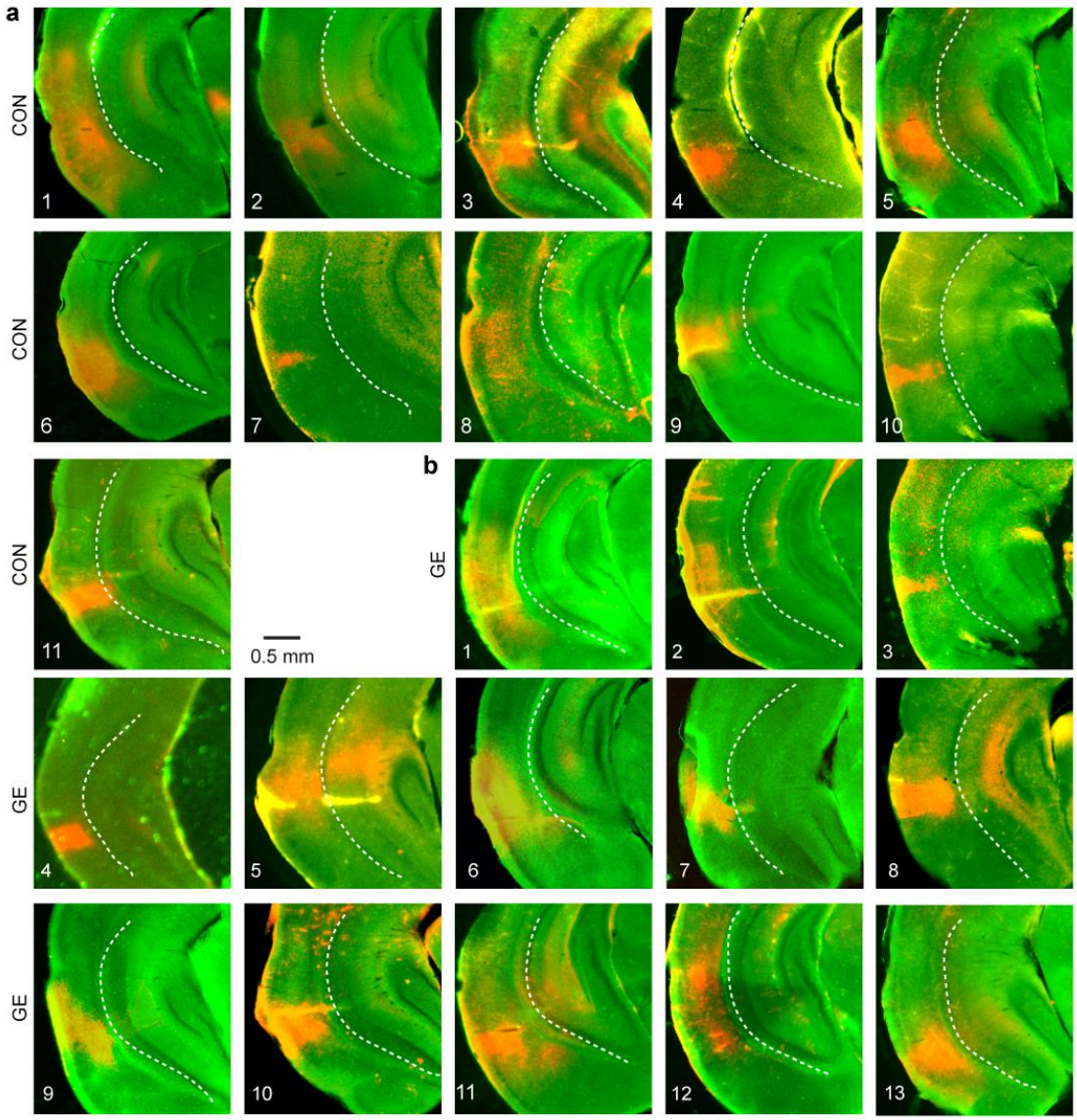

Supplementary fig.6 The injection position of AAV9-CaMKII-ChR2-mCherry in LEC for all the mice. (a) Photographs depicting the injection position for all CON mice used in the study. **(b)** Photographs depicting the injection position for all GE mice used in the study.

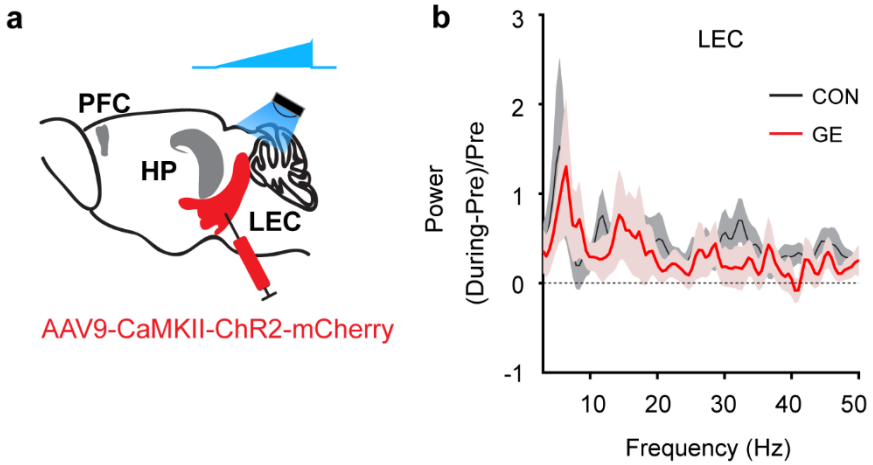

Supplementary fig.7 Oscillatory activity in response to light-induced activation of LEC. (a) Schematic of AAV9-CaMKII-ChR2-mCherry injection in the LEC activated by ramp light stimulation (blue). **(b)** Power of oscillatory activity in LEC during 3 s-long ramp stimulation of LEC pyramidal neurons normalized to the activity before the stimulation in CON and GE mice.